The power of one qubit in quantum simulation algorithms
Polla, S.

Citation

Polla, S. (2024, February 22). *The power of one qubit in quantum simulation algorithms. Casimir PhD Series*. Retrieved from https://hdl.handle.net/1887/3719849

Virtual mitigation of coherent non-adiabatic transitions by echo verification

5.1 Introduction

The study of quantum many-body systems requires the precise estimation of observables. Quantum state preparation is naturally a prerequisite to this end, which is the rationale behind quantum computers or quantum simulators. The adiabatic algorithm has demonstrated large success in a variety of platforms [175, 176]. Still, the performance of current devices is hindered by noise, which cannot be error corrected, yet. Therefore, error mitigation techniques have been explored both theoretically and experimentally and can significantly improve the estimation of observables [69, 79, 177]. Surprisingly, there have been few synergies jointly considering error mitigation for the adiabatic algorithm.

Any quantum circuit can be efficiently simulated by the adiabatic algorithm [178]. In adiabatic quantum computation, the system is initialized in the ground state of a trivial Hamiltonian and one seeks to prepare the ground state of the final Hamiltonian by slowly interpolating between the two. The success of the algorithm is determined by the speed of the adiabatic passage and spectral properties of the Hamiltonians [49, 179]. More precisely, the total evolution time, or circuit depth, depends inverse
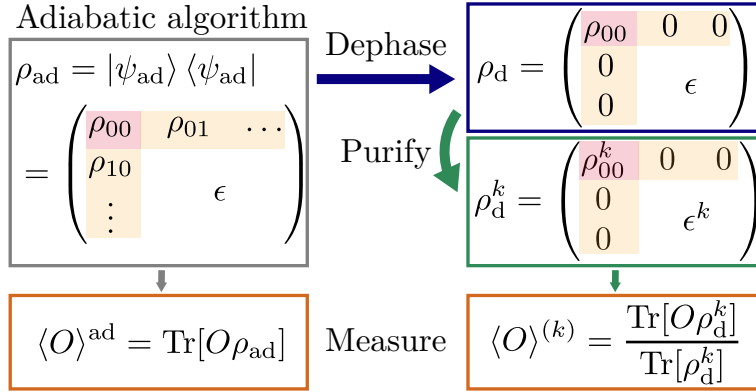
Figure 5.1: Schematic overview of the method. Density matrices are expressed in the energy eigenbasis of the target Hamiltonian. The pure state after the adiabatic evolution (ρ_{ad}) approximates the true ground state. Via a dephasing operation, the coherent error is promoted to an incoherent error in ρ_{d} such that error mitigation techniques can be applied. This allows measuring the kth degree purified observable $\langle O \rangle^{(k)}$ which yields a lower bias than evaluating the state directly after the adiabatic preparation $\left[\langle O \rangle^{\mathrm{ad}} \right]$.

polynomially on the minimum spectral gap between the ground state and the first excited state along the adiabatic path. These relations are quantified by the adiabatic theorem and versions thereof [51–53]. The adiabatic algorithm is especially suited for devices that implement dynamics natively without any Trotter overhead [180–183].

To address the restrictions in current hardware, various error mitigation techniques have been explored in recent years to improve the usefulness of a noisy quantum computation [79]. These methods include zero-noise extrapolation, exploiting symmetry or purity constraints, and several other approaches. Here, we focus on purity methods, which aim to suppress stochastic errors by projecting the noisy state ρ onto the closest pure state, given by the dominant eigenvector of ρ.

The purification can in general be achieved by collective measurements of several copies of ρ, known as virtual state distillation [148] or error suppression by derangement [184]. Echo verification (EV) achieves this using two copies of ρ multiplexed in time, rather than in space [156–158]. In EV, a desired state is prepared, an observable is measured
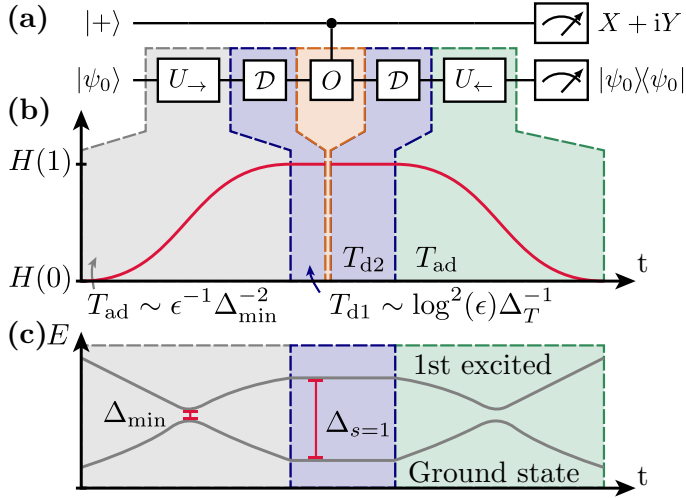
Figure 5.2: **(a)** Quantum circuit for adiabatic echo verification to estimate an observable $\langle O \rangle$. A quasi-adiabatic sweep $U_\rightarrow$ is followed by an approximate ground state dephasing operation $\mathcal{D}$. After the controlled application of a unitary observable O and dephasing again, the sweep is performed backward $U_\leftarrow (\neq U_\rightarrow^\dagger)$. Postprocessing the measurement result, including the success information of the ground state projection, allows to extract an improved expectation value. **(b)** Schematic of the Hamiltonian dynamics. Approximate dephasing is implemented by evolving with the target Hamiltonian at $s = 1$ for a random time. Typically, this time is much smaller than the time required for the adiabatic algorithm as depicted in **(c)**, where we sketch a corresponding low-energy spectrum.

controlled by an auxiliary qubit, and the state is then uncomputed. This allows to access expectation values of the so-called 2nd degree purified state of ρ: $\langle O \rangle_{\text{EV}} = \text{Tr}\big[O\rho^2\big] / \text{Tr}\big[\rho^2\big]$. Recently, purification-based error mitigation has been tested experimentally in the context of the variational quantum eigensolver [69]. Error mitigation methods tailored specifically to the adiabatic algorithm have been explored considerably less in the literature. Few exceptions consider error suppression and correction [185] or symmetry-protection for Trotter dynamics [186].

In this work, we present a mitigation technique for estimating observables on quasi-adiabatically-prepared states, in the spirit of echo verification (Fig. 5.1). Along with stochastic device noise, our method seeks to sup-

press the coherent error due to non-adiabatic transitions. Our method which we denote *Adiabatic Echo Verification* (AEV) relies on dephasing operations to promote the coherent errors to random errors, which can then be mitigated. Similar to the original echo verification technique, the leading order error in the ground state expectation value of an observable is suppressed quadratically. In particular, we consider an imperfect implementation of the dephasing operation using random-time evolution. Related random-time dynamics have been successfully used in the context of Zeno-type protocols [187]. The overhead from this dephasing operation is only poly-logarithmic in the accuracy of the dephasing operation for estimating observables of states within gapped phases. We discuss how the protocol compares favorably against doubling the total evolution time in the standard adiabatic algorithm. A key feature of our technique is that hardware noise is also mitigated naturally through the EV method. Our protocol only requires implementing positive-time evolution and applying the operator of interest in a controlled way. Hence, the protocol is not only suitable for purely gate-based quantum devices but also for hybrid quantum simulators, e.g. using neutral Rydberg atoms [182].

5.2 The adiabatic algorithm and purification-based error mitigation

In order to be able to measure observables on the ground state $|E_0\rangle$ of a target Hamiltonian H_T, a state approximating $|E_0\rangle$ with sufficient precision needs to be prepared. The quantum adiabatic algorithm (QAA) is a suitable algorithm for this task. At the heart of the QAA is the adiabatic theorem, which states that a system remains in an instantaneous eigenstate if the Hamiltonian is changed sufficiently slowly and the eigenstate is separated from other eigenstates by a minimum spectral gap $\Delta_{\min}$ throughout the transition [50]. Hence, the desired ground state $|\psi_T\rangle$ of a Hamiltonian of interest H_T can be prepared by interpolating from a suitable Hamiltonian H_0 with a trivial ground state $|\psi_0\rangle$ as

$$H(s) = (1 - s)H_0 + sH_T. \tag{5.1}$$

where $s = t/T$ is the parametrized time. The folk version of the adiabatic theorem states that a total time $T = \mathcal{O}\left(\Delta_{\min}^{-2}\epsilon^{-1/2}\right)$ suffices to prepare the ground state up to fidelity $1 - \epsilon$. Rigorous versions of the adiabatic theorem give a bound $T = \mathcal{O}\left(\Delta_{\min}^{-3}\epsilon^{-1/2}\right)$ if $H(s)$ is twice differentiable [51, 52]. Given a finite coherence time, the QAA prepares an approximation

to the target state $|\psi_{\mathrm{ad}}\rangle = \sqrt{1-\epsilon}\,|E_0\rangle + \sqrt{\epsilon}\,\big|E_0^{\perp}\big\rangle$ where $\langle E_0|E_0^{\perp}\rangle = 0$. Measuring an observable O, we obtain an approximation to the true value $\mathrm{Tr}\left[O\,|\psi\rangle\langle\psi|_{\mathrm{ad}}\right] = (1-\epsilon)\langle O\rangle_{|E_0\rangle} + \mathcal{O}(\sqrt{\epsilon})$.

Purification methods such as echo verification (EV) or virtual state distillation improve the quality of an expectation value measurement on a noisy (incoherent) approximation ρ of a pure state $|\psi\rangle\langle\psi|$. This is achieved by effectively measuring the expectation value $\mathrm{Tr}\left[O\rho^k\right]$ of O on the k-th power of the density matrix. Raising ρ to the k-th power suppresses the eigenvectors with smaller eigenvalues, increasing the relative weight of the dominant eigenvector which, for small enough noise, should be $|\psi\rangle$. As ρ^k is non-normalized, purification methods prescribe to independently measure $\mathrm{Tr}\left[\rho^k\right]$ to calculate the desired estimator

$$\langle O\rangle^{(k)} \coloneqq \mathrm{Tr}\left[O\rho^k\right] / \mathrm{Tr}\left[\rho^k\right]. \tag{5.2}$$

If ρ has an eigenstate $|E_0\rangle$ with large weight $c_0 = 1 - \epsilon$ (small positive ϵ), we can write the density matrix as $\rho = c_0\,|E_0\rangle\langle E_0| + \epsilon\rho_{\perp}$ with $\rho_{\perp}$ a density matrix orthogonal to $|E_0\rangle$ (i.e., $\rho_{\perp}\,|E_0\rangle = 0$). The kth degree purified estimator is then

$$\langle O\rangle^{(k)} = \frac{c_0^k\,\langle E_0|\,O\,|E_0\rangle + \epsilon^k\,\mathrm{Tr}\left[\rho_{\perp}^k O\right]}{c_0^k + \epsilon^k\,\mathrm{Tr}\left[\rho_{\perp}^k\right]} \tag{5.3}$$

$$= \langle E_0|\,O\,|E_0\rangle + \mathcal{O}(\epsilon^k\,\mathrm{Tr}\left[\rho_{\perp}^k\right]\|O\|), \tag{5.4}$$

where $\|\cdot\|$ is the operator norm. Echo verification implements purification for $k = 2$ using a single register by multiplexing two state-(un)preparation oracles in time. The method suppresses the error contributions $\mathcal{O}(\epsilon)$ such that the leading order becomes $\mathcal{O}(\epsilon^2)$.

5.3 Mitigating coherent errors in adiabatic state preparation

Our main contribution is to propose a method where the echo verification technique is applied to coherent errors. We focus on an application where the coherent error arises in the adiabatic algorithm due to finite algorithm runtimes. However, as the state prepared by a noiseless implementation of the adiabatic algorithm is pure, naive purification will not have any effect.

To recover the error mitigation power on $\rho_{\mathrm{ad}} = |\psi_{\mathrm{ad}}\rangle\langle\psi_{\mathrm{ad}}|$, we introduce

an ideal dephasing channel that turns coherent errors into incoherent noise,

$$\text{deph}_{H}[\rho] := \sum_{j} |E_j\rangle\langle E_j| \, \rho \, |E_j\rangle\langle E_j| = \text{diag}[\rho], \tag{5.5}$$

where we sum over an eigenbasis $\{|E_j\rangle\}_j$ of the target Hamiltonian H_T. Here, we assume a nondegenerate spectrum and give an extension for degenerate spectra in the Supplement. The dephasing channel projects a density matrix onto its diagonal in the energy eigenbasis, removing the off-diagonal coherences. Applying the channel to the state prepared by the adiabatic algorithm yields

$$\rho_{\text{d}} := \text{deph}_{H}[\rho_{\text{ad}}] = c_0 \, |E_0\rangle\langle E_0| + \epsilon \rho_\perp = \begin{pmatrix} c_0 & 0 & \dots & 0 \\ 0 & & & \\ \vdots & & \epsilon \rho_\perp & \\ 0 & & & \end{pmatrix} \tag{5.6}$$

with $\rho_\perp = \sum_{j \neq 0} \rho_{jj} \epsilon^{-1} |E_j\rangle\langle E_j|$. Then, using the echo verification technique on the dephased state, which is a mixed state, we obtain the following result for the observable O:

$$\frac{\text{Tr}[O\rho_{\text{d}}^k]}{\text{Tr}[\rho_{\text{d}}^k]} = (1 - \gamma) \langle E_0| O |E_0\rangle + \gamma \frac{\text{Tr}[O\rho_\perp^k]}{\text{Tr}[\rho_\perp^k]}, \tag{5.7}$$

with $\gamma = \left[1 + c_0^k / \left(\epsilon^k \, \text{Tr}[\rho_\perp^k]\right)\right]^{-1} \sim \mathcal{O}\left(\epsilon^k \, \text{Tr}[\rho_\perp^k]\right)$.

To implement echo verification, typically, an inverse pair of unitaries $(U_\rightarrow, U_\rightarrow^\dagger)$ would be required [156]. The unpreparation $U_\rightarrow^\dagger$ then uses negative-time dynamics, which is generally not available in analog simulators. For our purposes, however, we can consider the two states $\rho_{\text{ad}} = U_\rightarrow |\psi_0\rangle\langle\psi_0| U_\rightarrow^\dagger$ and $\sigma_{\text{ad}} = U_\leftarrow^\dagger |\psi_0\rangle\langle\psi_0| U_\leftarrow$, where $U_\leftarrow$ is a positive-time adiabatic evolution with an inverted schedule from $s = 1$ to $s = 0$ [cf. Fig. 5.2(b)]. Both states have the same guaranteed fidelity with the target state $|E_0\rangle$ from the adiabatic theorem and ground state coherences are surpressed after the dephasing operation. This allows to use positive-time dynamics for the unpreparation step in AEV.

Next, we consider the implementation of the dephasing channel. Importantly, we observe that a channel that dephases only the ground state would also be sufficient to achieve our goal, producing a state of the form Eq. 5.6 with a more general, non-diagonal $\rho_\perp$, provided that c_0 still dominates. In the following part, we analyze such an approximate dephasing operation using positive-time dynamics.

5.4 Implementation and cost of the dephasing

We can implement an approximation of the dephasing channel [Eq. 5.5] by a random-time evolution $\exp(-iH_T\tau)$, with τ sampled from a probability distribution $P(\tau)$, as follows: We limit the support of P to the interval $\tau \in [0, T_{\mathrm{d}}]$. This ensures the dephasing can be realized naturally in quantum simulators and limits the time overhead of the dephasing operation to $2\,T_{\mathrm{d}}$ for the AEV circuit. We define the approximate dephasing channel

$$\operatorname*{deph}_{H,P}[\rho] := \int_0^{T_{\mathrm{d}}} \mathrm{d}P(\tau) e^{-iH_T\tau} \rho e^{iH_T\tau} \tag{5.8}$$

$$= \sum_{j,k} \mathcal{F}_{jk} \, |E_j\rangle\!\langle E_j| \, \rho \, |E_k\rangle\!\langle E_k| \,, \tag{5.9}$$

where $\mathcal{F}_{jk} := \mathcal{F}[P](E_j - E_k)$ is the Fourier transform of the random-time distribution at the transition energies. We will make use of the shorthand $\mathcal{D}[\rho] := \operatorname{deph}_{H,P}[\rho]$. As we only need to dephase the ground state, we require $\max_{j>0} |\mathcal{F}_{0j}| < \delta$. Evaluating the adiabatic echo verification circuit (Fig. 5.2) with the *approximate* dephasing channel $\mathcal{D}[\rho]$ yields an estimator with expectation

$$\langle O \rangle^{\mathrm{AEV}} = \frac{\mathrm{Tr}[O\tilde{\rho}\tilde{\sigma}]}{\mathrm{Tr}[\tilde{\rho}\tilde{\sigma}]} \tag{5.10}$$

where $\tilde{\rho}_{jk} = \mathcal{F}_{jk}[\rho_{\mathrm{ad}}]_{jk}$ and $\tilde{\sigma}_{kl} = \mathcal{F}_{kl}^*[\sigma_{\mathrm{ad}}]_{kl}$, expressed as matrix elements in the eigenbasis of the target Hamiltonian (cf. Supplement). We can bound the deviation of the AEV estimator from the ground state expectation value as

$$\left| \langle O \rangle^{\mathrm{AEV}} - \langle E_0| \, O \, |E_0\rangle \right| \lesssim \|O\|(\epsilon^{1/2}\delta + \epsilon^2) \tag{5.11}$$

with a small prefactor. To ensure this error is bounded by $\mathcal{O}(\epsilon^2)$, it is then sufficient to take $\delta \sim \epsilon^{3/2}$.

An upper bound on the $|\mathcal{F}_{0j}|$ can be obtained as a functional of the distribution $P(\tau)$. We can thus redefine

$$\delta := \max_{\Delta > \Delta_T} \left| \mathcal{F}[P](\Delta) \right| \tag{5.12}$$

where $\Delta_T < E_1 - E_0$ is a lower bound on the target Hamiltonian ground state gap. In principle, different distributions can be chosen. We might, for example, simply choose a uniform distribution $P(\tau) = 1/T_{\mathrm{d}}$ for $\tau \in [0, T_{\mathrm{d}}]$. As its Fourier transform is the cardinal sine function $\sin(x)/x$, we obtain

$\delta \sim (\Delta T_{\mathrm{d}})^{-1}$. However, discontinuities in P or its derivatives limit the asymptotic decay of $\mathcal{F}[P]$ to a polynomial. We can improve upon this without increasing the maximal evolution time by choosing a mollifier, i.e. a smooth distribution supported on $[0, T_{\mathrm{d}}]$. A suitable example for our purposes is the rescaled bump function

$$P_{T_{\mathrm{d}}}(\tau) = \begin{cases} \frac{2}{\mathcal{N} T_{\mathrm{d}}} \exp\left[\frac{T_{\mathrm{d}}^2}{4\tau(\tau - T_{\mathrm{d}})}\right] & \text{if} \quad \tau \in [0, T_{\mathrm{d}}], \\ 0 \quad \text{otherwise}, \end{cases} \tag{5.13}$$

where $\mathcal{N} \approx 2.25$ is a normalization factor. The Fourier transform of this function decays super-polynomially. Adapting the results from Ref. 188, we recover

$$\delta < \sqrt{\frac{8\pi}{\sqrt{e}}} \, (T_{\mathrm{d}} \Delta_T)^{-3/4} \exp\left[-\sqrt{T_{\mathrm{d}} \Delta_T / 2}\right], \tag{5.14}$$

with the full derivation included in the Supplement. A dephasing time $T_{\mathrm{d}} \sim \Delta_T^{-1} \log^2[\epsilon]$ is thus sufficient to achieve an overall error $\mathcal{O}(\epsilon^2)$. Often, one is interested in observables of states in gapped phases [189], such that only the poly-logarithmic term contributes to a non-constant overhead.

5.5 Comparison with standard adiabatic algorithm.

We seek to compare the method proposed here with the trivial alternative for improving the performance of the adiabatic algorithm, which is simply doubling the evolution time in the QAA. In the standard adiabatic theorem, there is a polynomial relationship between the accuracy and the evolution time [51]. In principle, the adiabatic theorem can be improved towards an exponential error dependence by assuming a sufficiently smooth schedule with vanishing derivatives at the beginning and end of the schedule [53]. However, this is at the cost of passing the minimal spectral gap at a faster rate, which, in general, leads to more transitions. In practice, we can observe an exponential scaling (*Landau-Zener* regime) transitioning into an inverse-quadratic scaling for longer times [190].

Regarding our method, we therefore conclude that if the error dependence was indeed exponential, as in a Landau-Zener problem, the AEV would yield a performance comparable to the QAA with double the evolution time. Compared to the standard theorems with a polynomial dependence, our method improves up to quadratically. For the sake of
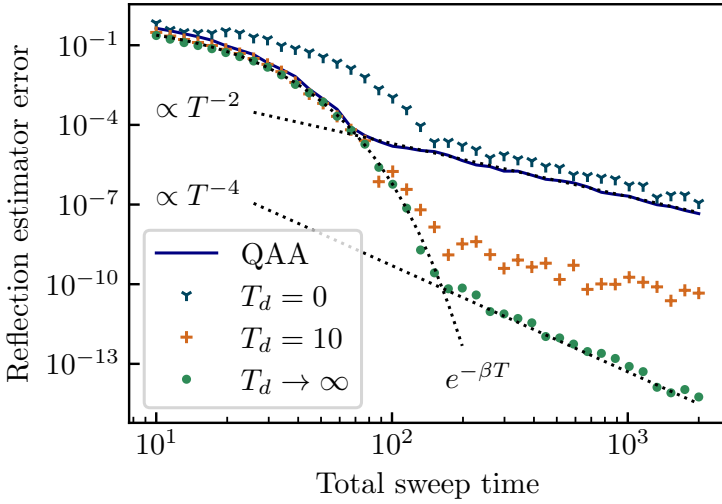
Figure 5.3: Comparing the QAA and AEV for different dephasing times T_{d}, as a function of the total sweep time T (QAA: $T = T_{\mathrm{ad}}$, AEV: $T = 2\,T_{\mathrm{ad}}$). AEV improves over simply doubling the QAA sweep time in the regime of polynomial error dependence. The respective estimator bias from $\langle E_0 | O | E_0 \rangle$ is shown, where $O = 1 - 2\,|E_0\rangle\langle E_0|$ is a reflection on the target state. The target Hamiltonian is an Ising model $H_T = 0.2 \sum_{j=1}^{5} \sigma_j^z - \sum_{j=1}^{4} \sigma_j^z \sigma_{j+1}^z$, and $H_0 = \sum_{j=1}^{5} \sigma_j^x$, using a linear schedule. We perform density-matrix simulations; time-dependent evolution is implemented by Euler integration, ensuring a sufficiently small error when discretizing the sweep. Approximate dephasing is implemented with $P(\tau)$ as in Eq. 5.13.

concreteness, we include numerical benchmarks in Fig. 5.3 showing an advantage for preparing the ground state of a transverse field Ising model.

5.6 Discussion and practical considerations.

In this letter, we introduced *Adiabatic Echo Verification* (AEV), a scheme to mitigate the coherent errors that characterize adiabatic state preparation. Our method is tailored to current quantum devices, which lack the possibility to correct errors. AEV requires doubling the circuit time compared to standard adiabatic state preparation, but improves up to

quadratically in the estimator bias. The additional features of the protocol are the following. First, in order to implement the verification part of the circuit, the path of the quasi-adiabatic evolution is simply reversed. Moreover, we show how the dephasing operation can be approximately implemented with positive-time dynamics. Hence, only positive-time evolution is required in AEV. This makes our method suitable for quantum computers that operate in a hybrid mode of digital gates and analog simulation. Rydberg atom arrays have recently demonstrated such capabilities [182, 191]. Additionaly, AEV naturally mitigates non-coherent hardware noise through echo verification. While our focus in the paper was not on the technical analysis of hardware noise mitigation, the results in echo verification literature fully apply to our case [69, 156].

We note that our method is compatible with arbitrary sweep profiles in the QAA. This is especially helpful as it is well known that slowing down the adiabatic sweep at the position of the minimum spectral gap mitigates transitions out of the ground state [192, 193]. More generally, our technique can be applied to other coherent approximate state preparation approaches, such as variational quantum algorithms (VQAs) [194]. This applies to VQAs that prepare a pure state heuristically by a parametrized operation $U(\theta)$ aiming at approximating the desired ground state. By dephasing the prepared state and using the echo verification technique, unpreparing the state with $U(\theta)^{\dagger}$, we expect that the performance of VQAs can be improved.

We note that the control-free versions of echo verification [69, 156], which employ a reference state instead of a control qubit, are not naively available for AEV. This is due the dephasing channel annihilating coherences between the reference state and the state of interest. Recently, a method for rescaling survival probabilities was considered that has similarities with control-free echo verification [195]. While their unnormalized estimator $\mathrm{Tr}\big[\rho O \rho O^{\dagger}\big]$ differs from the echo verification counterpart $\mathrm{Tr}\big[O\rho^2\big]$, it would still allow for mitigating errors for certain interesting observables such as out-of-time-order correlators (OTOCs) [146]. Not requiring the implementation of a controlled operation can significantly simplify experiments. This is why an extension of AEV without a control qubit is an interesting direction for future work. Another promising research direction is the combination of AEV with other purification-based error mitigation methods such as virtual state distillation [148, 184]. Using multiple copies of the quasi-adiabatically prepared state, further improvements for surpressing errors seem possible.

5.A Dephasing operation on a degenerate spectrum

In Eq. 5.5 we define the perfect dephasing channel for an operator H with non-degenerate spectrum. If the spectrum of H contains degeneracies, the dephasing channel will project ρ to a block-diagonal operator, where the blocks are defined by the (degenerate) eigenspaces of H:

$$\underset{H}{\mathrm{deph}}[\rho] = \sum_j \Pi_j \rho \Pi_j \tag{5.15}$$

where $\Pi_j = \delta(H - E_j)$ is the projector on the eigenspace of H with eigenvalue E_j.

For AEV, we are only interested in dephasing the ground state with respect to the rest of the spectrum; we only require the ground state of H to be non-degenerate for Eq. 5.6 and the subsequent analysis to be valid. This is anyway a typical requirement in adiabatic state preparation.

5.B Evaluation of AEV estimator with approximate dephasing

In this section, we evaluate the error on the Adiabatic Echo Verification (AEV) estimator with respect to the target value $\langle E_0 | O | E_0 \rangle$. We bound it as a function of the adiabatic state (un)preparation error ϵ and the dephasing approximation error δ. The AEV circuits we consider only require positive-time evolution with respect to the adiabatic Hamiltonian Eq. 5.1, and the ability to perform a controlled-O operation (or a decomposition thereof) to implement the Hadamard test.

We recall the echo verification (EV) expectation value estimator [69, 196] is defined as

$$\langle O \rangle^{\mathrm{EV}} := \frac{\mathbb{E}[\text{verified Hadamard test circuit (VHT)}]}{\mathbb{E}[\text{echo circuit (Echo)}]}. \tag{5.16}$$

In our case, the verified Hadamard test circuit is

$$\text{VHT} := \quad \begin{array}{c} |+\rangle \\ |\psi_0\rangle \end{array} \begin{array}{|c|c|c|c|c|} \hline U_\rightarrow & \mathcal{D} & O & \mathcal{D} & U_\leftarrow \\ \hline \end{array} \begin{array}{c} X + \mathrm{i}Y \\ |\psi_0\rangle\langle\psi_0| \end{array} \quad ,$$

(5.17)

where $U_\rightarrow$ is the adiabatic state preparation, $U_\leftarrow$ is the state unpreparation, and deph $:=$ deph$_{H,P}$ is the approximate dephasing. At the end of the circuit we need to measure $X \otimes |\psi_0\rangle\langle\psi_0|$ and $Y \otimes |\psi_0\rangle\langle\psi_0|$ to recover the real $\text{Re}[\langle O\rangle^{\text{EV}}]$ and imaginary $\mathrm{i}\,\text{Im}[\langle O\rangle^{\text{EV}}]$ parts of the expectation value, respectively. The output of a single sample of the circuit will be the result of the Pauli X (± 1) or Y ($\pm \mathrm{i}$) on the control qubit if the system register returns to the state $|\psi_0\rangle$, and 0 otherwise. Our notation supposes that O is a unitary operator, and its application is controlled by the state of the control qubit. If O is not unitary, we can rewrite it as a decomposition $O = \sum_x a_x \text{Re}[U_x] + b_x \text{Im}[U_x]$ and measure the terms of the decomposition separately [196]. The echo circuit, which is used to compute the normalization of $\langle O\rangle^{\text{EV}}$, is given as

$$\text{Echo} := \quad |\psi_0\rangle \begin{array}{|c|c|c|c|} \hline U_\rightarrow & \mathcal{D} & \mathcal{D} & U_\leftarrow \\ \hline \end{array} \begin{array}{c} |\psi_0\rangle\langle\psi_0| \end{array} \qquad (5.18)$$

and obtained by substituting the operator O with the identity in the previous circuit.

The adiabatic preparation and the adiabatic unpreparation are defined as

$$U_\rightarrow = \mathcal{T} \exp\left\{ -\mathrm{i} \int_0^{T_{\text{ad}}} H[s(t)]\, \mathrm{d}t \right\}; \qquad (5.19)$$

$$U_\leftarrow = \mathcal{T} \exp\left\{ -\mathrm{i} \int_0^{T_{\text{ad}}} H[s(T_{\text{ad}} - t)]\, \mathrm{d}t \right\}, \qquad (5.20)$$

where $\mathcal{T}\exp$ notates the time-ordered exponential, $H(s)$ is the adiabatic Hamiltonian (5.1), $s(t)$ the adiabatic schedule with $s(0) = 0$ and $s(T_{\text{ad}}) = 1$, and T_{ad} is the total evolution time of the adiabatic algorithm. Note that $\mathrm{d}t$ is always positive, thus negative-time evolution is not required to implement $U_\rightarrow$ and $U_\leftarrow$. Typically, in an EV circuit, if the preparation unitary is U, then the unpreparation is performed with its conjugate transpose $U^\dagger$ such

that $UU^\dagger = \mathbb{1}$. Here, however, this is not the case for the two operations $U_\leftarrow$ and $U_\rightarrow$. We will show that the added dephasing indeed removes this requirement for our purposes.

In our calculations, we only assume that $U_\rightarrow$ $(U_\leftarrow)$ implement an approximate state (un)preparation of $|E_0\rangle$ with a fidelity of at least $1 - \epsilon$ with small $\epsilon > 0$. Concretely, we define

$$|\langle E_0| U_\rightarrow |\psi_0\rangle|^2 = 1 - \epsilon_\leftarrow, \quad |\langle \psi_0| U_\leftarrow |E_0\rangle|^2 = 1 - \epsilon_\rightarrow, \quad (5.21)$$

such that $\epsilon = \max\{\epsilon_\leftarrow, \epsilon_\rightarrow\}$. It is reasonable to assume the two adiabatic processes will have a similar error, as any adiabatic theorem bounds both in the same way.

The approximate dephasing channel, of the form Eq. 5.8, is defined via a matrix of Fourier coefficients

$$\mathcal{F}_{jk} := \mathcal{F}[P](E_j - E_k) \in \mathbb{C}, \quad \mathcal{D}[\rho]_{jk} = \mathcal{F}_{jk}\rho_{jk} \quad (5.22)$$

We denote $A_{jk} = \langle E_j| A |E_j\rangle$ the matrix elements of an operator in the eigenbasis of H_T.

The only requirement on the dephasing channel is that the Fourier coefficients are bounded $\max_{j>0} |\mathcal{F}_{0j}| < \delta$, which imposes that the coherences between the ground state and any other eigenstate are suppressed by a factor smaller than δ. In the main text, we relate this factor to the dephasing time and to ground state gap of the target Hamiltonian.

The expectation value of circuit Eq. 5.17 is

$$\mathbb{E}[\text{VHT}] = \text{Tr}\left\{ U_\leftarrow \mathcal{D}\Big[\text{Ctrl}O\, \mathcal{D}[U_\rightarrow(|+\rangle\langle+| \otimes |\psi_0\rangle\langle\psi_0|)U_\rightarrow^\dagger]\text{Ctrl}O^\dagger\Big] \right.$$
$$\left. U_\leftarrow^\dagger \left(|\psi_0\rangle\langle\psi_0| \otimes 2|0\rangle\langle1|\right) \right\} =$$

$$= \text{Tr}\left\{ \underbrace{U_\leftarrow^\dagger |\psi_0\rangle\langle\psi_0| U_\leftarrow}_{\sigma}\, \mathcal{D}\Big[O\, \mathcal{D}[\, \underbrace{U_\rightarrow |\psi_0\rangle\langle\psi_0| U_\rightarrow^\dagger}_{\rho} \,] \Big] \right\} =$$

$$= \sum_{jk} \mathcal{F}_{jk}\, \text{Tr}\left\{ U_\leftarrow^\dagger |\psi_0\rangle\langle\psi_0| U_\leftarrow \cdot \right.$$
$$\left. \cdot \mathcal{D}\Big[O |E_j\rangle \underbrace{\langle E_j| U_\rightarrow |\psi_0\rangle\langle\psi_0| U_\rightarrow^\dagger |E_k\rangle}_{\rho_{jk}} \langle E_k| \Big] \right\} =$$

$$= \sum_{jkl} \mathcal{F}_{jk}\mathcal{F}_{lk}\sigma_{kl}\, O_{lj}\, \rho_{jk} \quad (5.23)$$

where we expand the dephasing channels, and we define the density matrices ρ and σ, corresponding respectively to the pure states

$$U_{\rightarrow} |\psi_0\rangle = \sqrt{1-\epsilon} |E_0\rangle + \sqrt{\epsilon} \sum_{j>0} \alpha_j |E_j\rangle \,, \quad \sum_{j>0} |\alpha_j|^2 = 1; \quad (5.24)$$

$$\langle\psi_0| U_{\leftarrow} = \sqrt{1-\epsilon} \langle E_0| + \sqrt{\epsilon} \sum_{j>0} \beta_j^* \langle E_j| \,, \quad \sum_{j>0} |\beta_j|^2 = 1. \quad (5.25)$$

We can then absorb the dephasing coefficients into $\tilde{\rho}_{jk} = \mathcal{F}_{jk}\rho_{jk}$ and $\tilde{\sigma}_{kl} = \mathcal{F}_{lk}\sigma_{kl} = \mathcal{F}_{lk}^*\sigma_{kl}$, simplifying

$$\mathbb{E}[\text{VHT}] = \text{Tr}[\tilde{\rho}\tilde{\sigma}O] \,, \quad \mathbb{E}[\text{Echo}] = \text{Tr}[\tilde{\rho}\tilde{\sigma}] \,, \quad \langle O \rangle^{\text{EV}} = \frac{\text{Tr}[\tilde{\rho}\tilde{\sigma}O]}{\text{Tr}[\tilde{\rho}\tilde{\sigma}]}. \quad (5.26)$$

Comparing this result to the standard purification estimator Eq. 5.2, we see that the ρ^2 is substituted by $\tilde{\rho}\tilde{\sigma}$. The explicit expression for this operator in the H_{T} eigenbasis is

$$
\begin{aligned}
\tilde{\rho}\tilde{\sigma} =& \left[(1-\epsilon)^2 + \epsilon(1-\epsilon) \sum_{j>0} \alpha_j^* \beta_j \mathcal{F}_{j0}^* \mathcal{F}_{0j} \right] |E_0\rangle \langle E_0| \\
&+ \sqrt{\epsilon}\sqrt{1-\epsilon} \sum_{j>0} \left[(1-\epsilon)\alpha_j \mathcal{F}_{j0} + \epsilon \sum_{l>0} \alpha_j \alpha_l^* \beta_l \mathcal{F}_{jl} \mathcal{F}_{l0}^* \right] |E_j\rangle \langle E_0| \\
&+ \sqrt{\epsilon}\sqrt{1-\epsilon} \sum_{j>0} \left[(1-\epsilon)\beta_j^* \mathcal{F}_{j0} + \epsilon \sum_{l>0} \beta_j^* \alpha_l^* \beta_l \mathcal{F}_{jl} \mathcal{F}_{l0}^* \right] |E_0\rangle \langle E_j| \\
&+ \epsilon \sum_{j,k>0} \left[(1-\epsilon)\alpha_j \beta_k^* \mathcal{F}_{j0} \mathcal{F}_{0k}^* + \epsilon \sum_{l>0} \alpha_j \alpha_l^* \beta_l \beta_k^* \mathcal{F}_{jl} \mathcal{F}_{lk}^* \right] |E_j\rangle \langle E_k| \\
=& [\tilde{\rho}\tilde{\sigma}]_{00} |E_0\rangle \langle E_0| + \sum_{j>0} [\tilde{\rho}\tilde{\sigma}]_{j0} |E_j\rangle \langle E_0| + \\
&+ \sum_{j>0} [\tilde{\rho}\tilde{\sigma}]_{0j} |E_0\rangle \langle E_j| + \sum_{j,k>0} [\tilde{\rho}\tilde{\sigma}]_{jk} |E_j\rangle \langle E_k| \,. \quad (5.27)
\end{aligned}
$$

We proceed by bounding the error of $\langle O \rangle^{\text{EV}}$ with respect to the target $\langle E_0| O |E_0\rangle$,

$$
\begin{aligned}
\text{error} :=& \left| \frac{\text{Tr}[O\tilde{\rho}\tilde{\sigma}]}{\text{Tr}[\tilde{\rho}\tilde{\sigma}]} - \langle E_0| O |E_0\rangle \right| \\
=& \left| \text{Tr}[O\tilde{\rho}\tilde{\sigma}] - O_{00} \text{Tr}[\tilde{\rho}\tilde{\sigma}] \right| \cdot \left| \text{Tr}[\tilde{\rho}\tilde{\sigma}] \right|^{-1}. \quad (5.28)
\end{aligned}
$$

In the H_T eigenbasis, the relevant terms read

$$\text{Tr}[O\tilde{\rho}\tilde{\sigma}] = [\tilde{\rho}\tilde{\sigma}]_{00}O_{00} + \sum_{j>0}[\tilde{\rho}\tilde{\sigma}]_{0j}O_{j0} + \sum_{k>0}[\tilde{\rho}\tilde{\sigma}]_{k0}O_{0k} + \sum_{j,k>0}[\tilde{\rho}\tilde{\sigma}]_{jk}O_{kj},$$

$$(5.29)$$

$$\text{Tr}[\tilde{\rho}\tilde{\sigma}] = [\tilde{\rho}\tilde{\sigma}]_{00} + \sum_{j>0}[\tilde{\rho}\tilde{\sigma}]_{jj}. \tag{5.30}$$

We focus first on bounding the first factor on the right-hand side of Eq. 5.28,

$$\left|\text{Tr}[O\tilde{\rho}\tilde{\sigma}] - O_{00}\text{Tr}[\tilde{\rho}\tilde{\sigma}]\right| = \left|\text{Tr}[(O - O_{00})\tilde{\rho}\tilde{\sigma}]\right|. \tag{5.31}$$

We separate this expression through the triangle inequality,

$$\left|\text{Tr}[O\tilde{\rho}\tilde{\sigma}] - O_{00}\text{Tr}[\tilde{\rho}\tilde{\sigma}]\right| =$$

$$= \left|\sum_{j>0}[\tilde{\rho}\tilde{\sigma}]_{0j}O_{j0} + \sum_{k>0}[\tilde{\rho}\tilde{\sigma}]_{k0}O_{0k} + \sum_{j,k>0}[\tilde{\rho}\tilde{\sigma}]_{jk}O_{kj} - \sum_{j>0}[\tilde{\rho}\tilde{\sigma}]_{jj}O_{00}\right|$$

$$\leq \|O\|\left(\left|\sum_{j>0}[\tilde{\rho}\tilde{\sigma}]_{0j}\right| + \left|\sum_{j>0}[\tilde{\rho}\tilde{\sigma}]_{j0}\right|\right) + \left|\sum_{j,k>0}[\tilde{\rho}\tilde{\sigma}]_{jk}O_{kj} - \sum_{j>0}[\tilde{\rho}\tilde{\sigma}]_{jj}O_{00}\right|,$$

$$(5.32)$$

where $\|\cdot\|$ is the operator norm. To bound the first term, we apply again the triangle inequality,

$$\left|\sum_{j>0}[\tilde{\rho}\tilde{\sigma}]_{0j}\right| \leq \left|\sum_{j>0}\tilde{\rho}_{00}\tilde{\sigma}_{0j}\right| + \left|\sum_{j,k>0}\tilde{\rho}_{0k}\tilde{\sigma}_{kj}\right| \tag{5.33}$$

and bound both resulting terms through Cauchy-Schwartz inequalities,

$$\left|\sum_{j>0}\tilde{\rho}_{00}\tilde{\sigma}_{0j}\right| \leq (1-\epsilon)^{3/2}\,\epsilon^{1/2}\left|\sum_{j}\mathcal{F}_{j0}\beta_j^*\right|$$

$$\leq (1-\epsilon)^{3/2}\,\epsilon^{1/2}\,|\vec{\beta}|\,\max_{k>0}|\mathcal{F}_{0k}| = (1-\epsilon)^{3/2}\,\epsilon^{1/2}\delta; \tag{5.34}$$

5

169

$$\left| \sum_{j,k>0} \tilde{\rho}_{0k}\, \tilde{\sigma}_{kj} \right| = (1-\epsilon)^{1/2}\, \epsilon^{3/2} \left| \sum_{j,k>0} \mathcal{F}_{0k}\alpha_k^*\beta_k \mathcal{F}_{jk}\beta_j^* \right|$$

$$\leq (1-\epsilon)^{1/2}\, \epsilon^{3/2}\, |\vec{\beta}| \sum_{j>0} \left| \sum_{k>0} \mathcal{F}_{jk}\alpha_k^*\beta_k \mathcal{F}_{0k} \right|$$

$$\leq (1-\epsilon)^{1/2}\, \epsilon^{3/2}\, |\vec{\beta}|^2\, |\vec{\alpha}| \max_{j,k>0} |\mathcal{F}_{jk}| \max_{k>0} |\mathcal{F}_{0k}|$$

$$\leq (1-\epsilon)^{1/2}\, \epsilon^{3/2}\delta \tag{5.35}$$

where we note that $\vec{\alpha}$ and $\vec{\beta}$ are normalized by defintion, $\mathcal{F}_{jk} \leq 1$ and $\max_{k>0} |\mathcal{F}_{0k}| = \delta$. The same bound applies to the second term in the parentheses in Eq. 5.32, $\left| \sum_{j>0}[\tilde{\rho}\tilde{\sigma}]_{j0} \right|$. The last term of Eq. 5.32 can be rewritten as

$$\sum_{j,k>0} [\tilde{\rho}\tilde{\sigma}]_{jk}O_{kj} - \sum_{j>0}[\tilde{\rho}\tilde{\sigma}]_{jj}O_{00} = \text{Tr}[\Pi_> \tilde{\rho}\tilde{\sigma}\, \Pi_> (O - O_{00}\mathbb{1})] \tag{5.36}$$

where $\Pi_> = \mathbb{1} - |E_0\rangle\langle E_0|$ is the projector on the subspace orthogonal to $|E_0\rangle$. We can then use the Von Neumann inequality to bound

$$\left| \text{Tr}[\Pi_> \tilde{\rho}\tilde{\sigma}\, \Pi_> (O - O_{00}\mathbb{1})] \right| \leq \|O - O_{00}\mathbb{1}\| \cdot \|\Pi_> \tilde{\rho}\tilde{\sigma}\, \Pi_>\|_1 \tag{5.37}$$

where $\|A\|_1 = \text{Tr}\sqrt{A^\dagger A}$ is the trace norm.

Now, by virtue of the triangle inequality, and the fact that $\| |u\rangle\langle v| \|_1 = \|u\|\|v\|$, for any vectors $|u\rangle, |v\rangle$, we have

$$\|\Pi_>\tilde{\rho}\tilde{\sigma}\Pi_>\|_1 \leq \epsilon(1-\epsilon) \left\| \sum_{j>0} \alpha_j \mathcal{F}_{j0} |E_j\rangle \right\| \left\| \sum_{k>0} \beta_k \mathcal{F}_{0k} |E_k\rangle \right\| +$$

$$+ \epsilon^2 \sum_{l>0} |\alpha_l||\beta_l| \left\| \sum_{j>0} \alpha_j \mathcal{F}_{jl} |E_j\rangle \right\| \left\| \sum_{k>0} \beta_k \mathcal{F}_{lk} |E_k\rangle \right\|$$

$$\leq \epsilon(1-\epsilon)\delta^2 + \epsilon^2 \left(\max_{j,k>0} |\mathcal{F}_{jk}| \right)^2 \sum_{l>0} |\alpha_l||\beta_l|$$

$$\leq \epsilon(1-\epsilon)\delta^2 + \epsilon^2 \tag{5.38}$$

where we used Cauchy-Schwartz in the last line.

Combining the bounds from Eqs. (5.34), (5.35) and (5.38), and using

$\|O - O_{00}\mathbb{1}\| \le 2\|O\|$, we get

$$\left| \text{Tr}[O\tilde{\rho}\tilde{\sigma}] - O_{00}\,\text{Tr}[\tilde{\rho}\tilde{\sigma}] \right| \le$$
$$\le 2\|O\| \left[(1-\epsilon)^{3/2}\,\epsilon^{1/2}\delta + 3(1-\epsilon)^{1/2}\,\epsilon^{3/2}\delta + \epsilon(1-\epsilon)\delta^2 + \epsilon^2 \right]. \quad (5.39)$$

Next, to bound the factor $|\text{Tr}[\tilde{\rho}\tilde{\sigma}]|^{-1}$ in Eq. 5.28, we apply the reverse triangle inequality to $|\text{Tr}[\tilde{\rho}\tilde{\sigma}]|$:

$$\left| \text{Tr}[\tilde{\rho}\tilde{\sigma}] \right| = \left| (1-\epsilon)^2 + 2\epsilon(1-\epsilon)\,\text{Re}\left(\sum_{j>0} \alpha_j \beta_j^* \mathcal{F}_{j0}^2 \right) + \epsilon^2 \sum_{j,l>0} \alpha_j \alpha_l^* \beta_l \beta_j^* \mathcal{F}_{jl}^2 \right|$$
$$\ge \left| (1-\epsilon)^2 - 2\epsilon(1-\epsilon) - \epsilon^2 \right| \quad (5.40)$$

where we used that $\delta \le 1$. For $\epsilon < \sqrt{3/2} - 1$, the argument in Eq. 5.40 is strictly positive, so we can remove the absolute value signs. The dominant terms in the error Eq. 5.28 are then

$$\text{error} \sim \|O\|(\epsilon^{1/2}\delta + \epsilon^2). \quad (5.41)$$

We can verify that for $\delta \to 0$ we recover the error scaling with ϵ^2, as expected from perfect dephasing. To achieve the same scaling, it is in fact sufficient to choose $\delta = \epsilon^{3/2}$.

5.C Dephasing time for a smooth probability distribution

In this section we motivate the choice of the rescaled bump function in Eq. 5.13 for the distribution $P(\tau)$ used to implement dephasing by random-time evolution (Eq. 5.8). We recall that we require $P : [0, T_{\text{d}}] \to \mathbb{R}_+$ to have support on $[0, T_{\text{d}}]$. This ensures we only need to evolve for positive times and the maximal dephasing time is T_{d}. The performance for the dephasing operation on the ground state is measured by $\delta = \max_{\Delta > \Delta_T} |\mathcal{F}[P](\Delta)|$, which is essentially a bound on the decay of the Fourier transformation of P. As τ and Δ are conjugate dimensionful variables, we can equivalently study

$$\delta = \max_{\omega > \Delta_T T_{\text{d}}} |\mathcal{F}[\tilde{P}](\omega)| \quad \text{for} \quad \tilde{P} : [0, 1] \to \mathbb{R}_+, \quad (5.42)$$

where $\tilde{P}(\tau\Delta_T) = P(\tau)$.

To obtain the best possible asymptotic decay of the Fourier transform of a function $\mathcal{F}[f]$, we should choose f to be smooth. In fact, requiring the

Fourier transform of f to decay as $\mathcal{F}[f](k) \lesssim |k|^{-(r+1+\epsilon)}$ (for any choice of $\epsilon > 0$) implies that

$$\exists L_r > 0 : \forall x \quad \left| \frac{\mathrm{d}^r f(x)}{\mathrm{d}x^r} \right| = \left| \int \mathrm{d}k \, e^{ikt} \underbrace{k^r \mathcal{F}[f](k)}_{\lesssim |k|^{-(1+\epsilon)}} \right| < L_r, \qquad (5.43)$$

because $|k|^{-(1+\epsilon)}$ is absolutely integrable away from 0 and $\mathcal{F}[f](k)$ is bounded. This implies that f and all its derivatives up to order $r - 1$ are Lipschitz continuous. Thus, to achieve a Fourier transform decaying faster than any polynomial $\mathcal{F}[f](k) = o(1/\mathrm{poly}(k))$, we have to choose $f(x) \in C_\infty$ a smooth function.

One smooth function with compact support is the bump function

$$f(x) = \begin{cases} e^{-(1-x^2)^{-1}} & \text{if} \quad -1 < x < 1, \\ 0 & \text{otherwise}, \end{cases} \qquad (5.44)$$

we define its norm $\mathcal{N} := \int_{-1}^{1} f(x) \, \mathrm{d}x \approx 2.25$. Based on this function, we define the probability distribution

$$\begin{aligned} P_{T_\mathrm{d}}(\tau) &= \frac{2}{T_\mathrm{d} \mathcal{N}} f\left(2\frac{\tau}{T_\mathrm{d}} - 1 \right) \\ &= \begin{cases} \frac{2}{T_\mathrm{d} \mathcal{N}} \exp\left(\left[4(\frac{\tau}{T_\mathrm{d}} - 1)\frac{\tau}{T_\mathrm{d}} \right]^{-1} \right) & \text{if} \quad 0 < \tau < T_\mathrm{d}, \\ 0 & \text{otherwise}, \end{cases} \end{aligned} \qquad (5.45)$$

which is normalized, smooth, and has support on $[0, T_\mathrm{d}]$. The Fourier transform of this function can be estimated through the saddle point approximation; we build on the results of Ref. 188 which provide a bound the Fourier transform $\mathcal{F}[\mathcal{N} f]$ of the normalized $f(x)$:

$$\mathcal{F}[\mathcal{N} f](k) \approx 2 \, \mathrm{Re} \left[\sqrt{\frac{-i\pi}{\sqrt{2i}}} e^{ik - \frac{1}{4} - i\sqrt{k}} \right] k^{-\frac{3}{4}} e^{-\sqrt{k}}. \qquad (5.46)$$

We construct a monotonic envelope for this oscillating function by substituting the real part for an absolute value, and we perform a change of variables obtaining the bound

$$\delta = \max_{\Delta > \Delta_T} |\mathcal{F}[P_{T_\mathrm{d}}](\Delta)| < \sqrt{\frac{8\pi}{\sqrt{e}}} (T_\mathrm{d} \Delta_T)^{-3/4} e^{-\sqrt{T_\mathrm{d} \Delta_T / 2}}. \qquad (5.47)$$

The validity of this bound is also verified numerically. This translates to a statement on the dephasing time T_d required to achieve a target dephasing performance δ_target for a given gap Δ_T between the ground state and the first excited state of H_T. Note that the inverse is defined in terms of the principal branch W_0 of the Lambert W function. We obtain

$$T_\mathrm{d} = \frac{9}{2\,\Delta_T} W_0 \left[\frac{2\sqrt{2}\,\pi^{1/3}}{3\,e^{1/6}\,\delta_\mathrm{target}^{2/3}} \right] \lesssim O\left(\log^2(\delta_\mathrm{target}^{-1})\Delta_T^{-1} \right). \qquad (5.48)$$

Thus, T_d grows linearly with Δ_T and poly-logarithmically with $\delta_\mathrm{target}^{-1}$.

5